0026-895X/89/040495-09$02.00/0

MOLECULAR PHARMACOLOGY, 35:495-503

The Conformational Analysis of Δ^9- and $\Delta^{9,11}$-Tetrahydrocannabinols in Solution using High Resolution Nuclear Magnetic Resonance Spectroscopy

R. W. KRIWACKI[1] and A. MAKRIYANNIS

Section of Medicinal Chemistry and Pharmacognosy/Institute of Material Science, University of Connecticut, Storrs, Connecticut 06268

Received August 15, 1988; Accepted January 4, 1989

SUMMARY

The conformation for each of two cannabinoids, Δ^9-tetrahydrocannabinol (THC), the principal active constituent of marihuana, and $\Delta^{9,11}$-THC, a biologically inactive structural isomer of Δ^9-THC, is analyzed by interpreting ^{1}H-^{1}H and ^{13}C-^{1}H coupling constants and nuclear Overhauser effects determined using one- and two-dimensional ^{1}H and ^{13}C NMR techniques. The interpretation of both vicinal and long range coupling constants was necessary to deduce the conformations of these tricyclic molecules with certainty, with nuclear Overhauser effect enhancements used, when appropriate, to confirm the results. These findings provide insights into the structure-activity requirements for the cannabinoids.

The pharmacological properties and structure-activity relationships of cannabinoids are well documented in the literature (1–4). However, very little is understood regarding the relationship between the three-dimensional geometry of these molecules and their molecular mechanism of action. Efforts to probe this question are complicated by the fact that a specific receptor site responsible for the biological effects of the cannabinoids has not yet been clearly identified. Despite this lack of information for the cannabinoids, clear indications exist in the literature that molecular geometry plays an important role in determining the activity of these highly lipid-soluble molecules. For example, naturally occurring cannabinoid isomers, and synthetically and metabolically produced derivatives, are known to exhibit widely varying potencies (1). Within the family of THC isomers, Δ^9- and Δ^8-THC are highly active (1) whereas $\Delta^{9,11}$-THC is inactive (5). In this report we analyze the conformation of Δ^9-THC, the principal active constituent of marihuana, and $\Delta^{9,11}$-THC, the biologically inactive synthetic isomer of Δ^9-THC, and consider the geometry of each in the context of their disparate biological activities.

We used high field NMR spectroscopic methods to definitively determine the conformations of these two molecules. The analytical process involved first the complete assignment of the ^{1}H NMR spectra for each molecule using decoupling methods and 2D COSY. Secondly, we determined all interproton coupling constants relevant to the conformational analysis, especially vicinal ^{1}H-^{1}H coupling constants (^3J) between hydrogens of the aliphatic carbocyclic C ring (Fig. 1) 2D J-resolved ^{1}H NMR spectroscopy was used to separate the many overlapping multiplets and allowed the determination of approximate ^3J values, which were then refined through iterative simulation of subspectra containing only the resonances of the C ring. The conformation of each molecule was then determined first by interpreting the ^3J values in the context of the well known Karplus equation, which relates vicinal coupling constants with the corresponding dihedral angles (6). In addition, ^{13}C-^{1}H coupling constants and certain long range ^{1}H-^{1}H coupling constants, as well as ^{1}H-^{1}H nOe measurements, were used to confirm the above conclusions and to provide information on the conformation of the B ring and pentyl side-chain. The detailed conformational analysis of the THC isomers provides some insights into the molecular mode of cannabinoid action and provides a good starting point for the analysis of other analogs.

Experimental Procedures

Materials. Δ^9-THC (20%, w/v, in ethanol and $\Delta^{9,11}$-THC (pure gum) were obtained from the National Institute on Drug Abuse (Be-

This work was supported by a grant from the National Institute on Drug Abuse (DA-3801).

[1] Present address: Boehringer Ingelheim Pharmaceuticals, Inc., 90 East Ridge, Ridgefield, CT 06877.

ABBREVIATIONS: Δ^9-THC, (−)-Δ^9-6a,10a-*trans*-tetrahydrocannabinol; Δ^8-THC, (−)-Δ^8-6a,10a-*trans*-tetrahydrocannabinol; $\Delta^{9,11}$-THC, (−)-$\Delta^{9,11}$-6a,10a-*trans*-tetrahydrocannabinol; 1D, one-dimensional; 2D, two-dimensional; COSY, correlation spectroscopy; ^2J, geminal coupling constant through two bonds; ^3J, vicinal coupling constant through three bonds; ^4J, long range coupling constant through four bonds; ^5J, long range coupling constant through five bonds; nOe, nuclear Overhauser effect; $\Delta\nu_{1/2}$, line width at half peak height; TMS, tetramethylsilane; S/N, signal to noise ratio; $^3J(a\text{-}a)$, vicinal coupling constant between *trans* diaxial hydrogens in cyclohexane; $^3J(a\text{-}e)$, vicinal coupling constant between one axial hydrogen and one equatorial hydrogen in cyclohexane; ^3J(e-e), vicinal coupling constant between two equatorial hydrogens in cyclohexane.

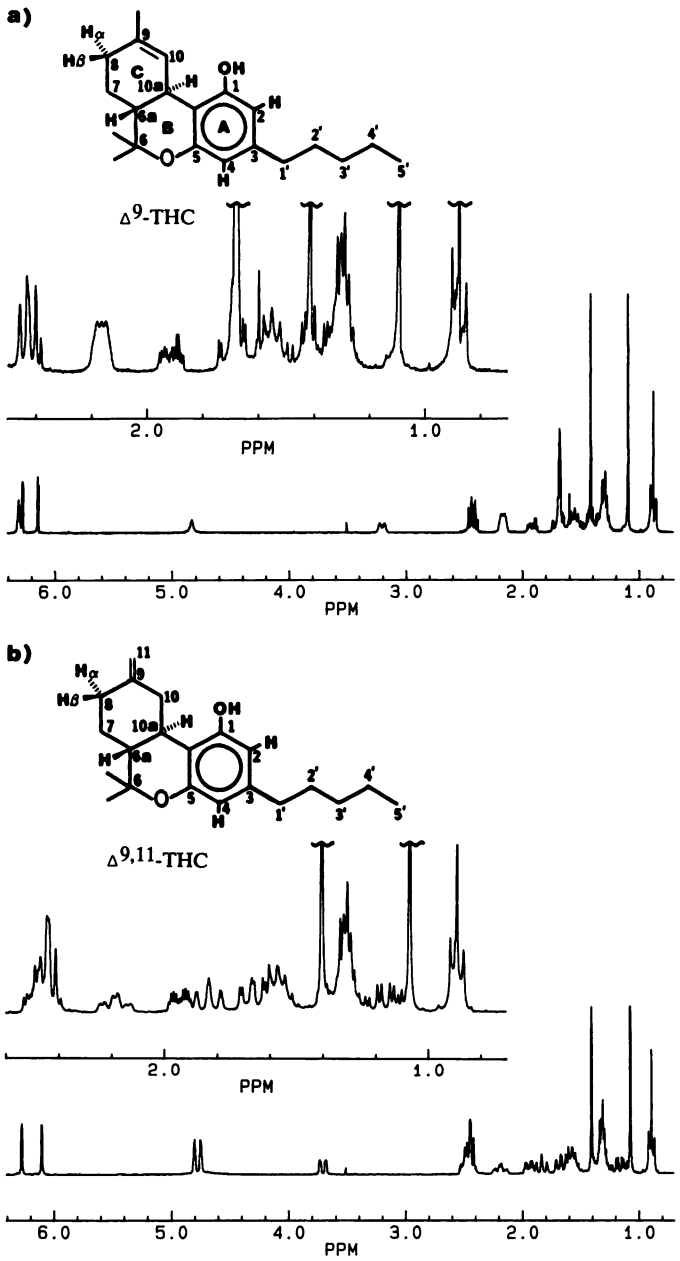

Fig. 1. Full scale and expanded scale 250 MHz ^{1}H NMR spectra of Δ^9-THC (a) and $\Delta^{9,11}$-THC (b) in $CDCl_3$.

thesda, MD). $CDCl_3$ and TMS were obtained from the Aldrich Chemical Company (Milwaukee, WI). Cannabinoids were dissolved in $CDCl_3$ (0.01 M for ^{1}H NMR, 0.5 M for ^{13}C NMR), degassed using several freeze-pump-thaw cycles, and sealed in high quality 5-mm NMR tubes (Wilmad Glass Co., Buena, NJ). TMS was used as an internal reference.

1D NMR spectra. Spectra at 250 MHz were obtained using a Bruker Instruments WM-250 pulsed FT NMR spectrometer under ASPECT 2000A control in the quadrature detection mode using a variable-temperature 5-mm ^{1}H probe with the following parameters: pulse width, 1 μsec (20° tip angle); spectral width, 2300 Hz (9.2 ppm); data size, 16k points; and recycle delay, 1 sec at 295° K. A total of 512 transients were required for an acceptable S/N. ^{1}H spectra at 500 MHz and 125 MHz ^{13}C spectra were obtained using a Bruker Instruments WM-500 pulsed FT NMR spectrometer under ASPECT 2000 control in the quadrature detection mode using variable-temperature 5-mm ^{1}H and ^{13}C probes. ^{1}H spectra at 500 MHz were obtained with the following parameters: pulse width, 8 μsec (45° tip angle); spectral width, 3700 Hz (7.4 ppm); data size, 32k points; and recycle delay, 1 sec at 300° K. A total of 48 transients were required for an acceptable S/N. ^{13}C spectra at 125 MHz were obtained with the following parameters: pulse width, 5 μsec (30° tip angle); spectral width, 20,000 Hz (160 ppm); data size, 32k points; and recycle delay, 2 sec at 300° K. A total of 100 transients were required for acceptable S/N when broadband ^{1}H decoupling was used. ^{1}H-coupled ^{13}C spectra were obtained using gated ^{1}H decoupling with the decoupler gated on during the recycle delay then gated off during acquisition. A total of 1000 transients were required for these spectra. Lorentzian or Gaussian filtering were applied to FIDs in certain cases before Fourier transformation and phase correction, to improve either the S/N or the effective spectral resolution.

^{1}H difference spectra. ^{1}H-decoupled difference spectra were obtained according to the experimental procedure of Hall and Sanders (7), calling for sequential acqusition and storage of eight transients with irradiation at each of several frequencies stored in a computer-held list. One frequency in the list corresponded to a blank region of the spectrum and was used as the control spectrum. This sequence was repeated 50 times to give a total of 400 transients stored per irradiation frequency. The irradiation frequency in the control spectrum was as close to the irradiated peaks as possible without causing perturbations in adjacent resonances. This condition minimizes the Block-Siegert effect. The stored FIDs were Fourier transformed, Lorentzian filtered, and phase corrected using identical normalization, line broadening (1–2 Hz), and phase constants. The control spectrum was subtracted from each decoupled spectrum to give the difference spectra. ^{1}H difference nOe spectra were also acquired using sequential acquisition; however, subsaturating preirradiation (1 sec) was used before acquisition. Preirradiation was gated off 2 msec before acquisition to eliminate decoupler turn-off artifacts. A 5-sec recycle delay was included after each transient to reestablish spin equilibrium. Eight FIDs were acquired and stored before moving to the next irradiation frequency. This cycle was repeated 100 times to give 800 transients per spectrum. The spectra were processed in the same manner as for the decoupling experiments.

Quantitation of nOe enhancements. nOe enhancements were quantitated by measuring the areas of peaks in both perturbed (with nOe) and control spectra. The nOe enhancement is reported as the percentage increase in peak area.

2D *J* spectroscopy. The 2D *J*-resolved ^{1}H spectra were acquired at 500 MHz using the 90°(ϕ_1)-t_1/2-180°(ϕ_2)-t_1/2-t_2 pulse sequence (8, 9) with Exorcycle (10) and Cyclops (11) phase cycling to eliminate pulse imperfections and quadrature channel imbalance, respectively; $\phi_1 \equiv x,x,x,x,y,y,y,y,-x,-x,-x,-x,-y,-y,-y,-y$; $\phi_2 \equiv x,y,-x,-y,y,-x,-y,x,-x,-y,x,y,-y,x,y,-x$, and the receiver was cycled, $x,-x,x,-x,y,-y,y,-y,-x,x,-x,x,-y,y,-y,y$. Typical acquisition parameters for this experiment were as follows: 90° pulse width, 14 μsec; initial value of $t_{1/2}$, 3 μsec; $t_{1/2}$ increment, 8 μsec; spectral width in f_1, 61.25 Hz; spectral width in f_2, 1000 Hz; and recycle delay, 2 sec. The data were $64w$ in f_1 and $2k$ in f_2 and were zero-filled to $128w \times 4k$ before 2D Fourier transformation. Data processing, including sine-bell apodization in both domains, 2D Fourier transformation, tilting, symmetrization, projection, and plotting was performed using the Bruker FTNMR2D software package. The final resolution in both frequency domains was 0.49 Hz/point. Data acquisition required approximately 3 hr with 64 transients stored per t_1 value. Sine-bell apodization was used in both time domains to reduce f_1 tails and to enhance the apparent spectral resolution in both frequency domains.

2D COSY. COSY spectra were acquired using the 90°(ϕ_3)-t_1-90°(ϕ_4)-t_2 pulse sequence (12) at 250 MHz. Phase cycling was optimized for N-type (coherence transfer echo) peak selection (13), axial peak suppression (13, 14), and elimination of quadrature channel imbalance (Cyclops) (11) where $\phi_3 \equiv x,x,x,x,y,y,y,y,-x,-x,-x,-x,-y,-y,-y,-y$; $\phi_4 \equiv x,y,-x,-y,y,-x,-y,x-x,-y,x,y,-y,x,y,-x$, and the receiver was cycled, $x,-x,x,-x,y,-y,y,-y,-x,x,-x,x,-y,y,-y,y$. Typical acquisition parameters for this experiment were as follows: 90° pulse width, 4.7 μsec; inital t_1 value, 3 μsec; t_1 increment, 333 μsec for Δ^9-THC (312 μsec for $\Delta^{9,11}$-THC); spectral width in f_1 and f_2, 1501.5 Hz for Δ^9-THC (1602.6 Hz for

$\Delta^{9,11}$-THC); and recycle delay, 1 sec at 295° K. The data were 256w in f_1 and 512w in f_2 and were zero-filled in f_1 before 2D Fourier transformation to 512w × 512w. 2D Fourier transformation, sine-bell apodization, and plotting were performed using Bruker's DISNMR software package. The data are presented in the absolute-value mode. Resolution in both frequency dimensions for Δ^9-THC was 1.47 Hz/point (1.57 Hz/point for $\Delta^{9,11}$-THC). A total of 128 transients were required for each t_1 value, giving a data acquisition time of approximately 12 hr. COSY spectra optimized for long range couplings were acquired using the pulse sequence 90°-t_1-Δ-90°-Δ-t_2 (15), in which the value of Δ (0.4 sec) was optimized for couplings on the order of 1–2 Hz. Other experimental and processing parameters were identical to those used in the normal COSY experiments above.

Results

Chemical Shift Assignments

Fig. 1a shows the 500 MHz ^{1}H NMR spectrum of Δ^9-THC. The partial assignments made by Archer *et al.* (16) at 90 MHz and 200 MHz for Δ^9-THC are included parenthetically in Table 1. Our studies confirm these assignments and provide assignments for the remaining resonances of the C ring (see Fig. 1). We have used two methods not used by the previous workers to assign all resonances in Δ^9-THC, namely difference decoupling techniques and 2D COSY. The side-chain hydrogens (1′–5′) were assigned, first, by comparison with assignments for *n*-pentyl benzene (17) (see Table 1) and, second, by analyzing the results of the decoupling and 2D COSY experiments. The aromatic and olefinic hydrogens, as a group, were assigned initially on the basis of chemical shift and were later specifically assigned on the basis of nOe experiments. The methyl resonances (6α, 6β, and 9) were identified in the spectrum as the broadened singlets integrating to three hydrogens each. The downfield methyl resonance was assigned as the 9-CH_3 based on the observation that this peak narrows when the olefinic hydrogen is decoupled. The 6α and 6β methyl groups were distinguished on the basis of nOe measurements.

TABLE 1

^{1}H NMR chemical shift assignments for Δ^9- and $\Delta^{9,11}$-THC in $CDCl_3$ solution at 295°K

Spectra were obtained at 500 MHz using TMS as internal reference.

Hydrogen	Chemical Shift	
	Δ^9-THC	$\Delta^{9,11}$-THC
2	6.18 (6.15)[a]	6.12
4	6.30 (6.29)	6.28
6a	1.72	1.68
6α-CH_3	1.12 (1.09)	1.08
6β-CH_3	1.47 (1.41)	1.40
7α	1.43	1.26
7β	1.93	1.96
8α	2.20	2.50
8β	2.20	2.20
9-CH_3	1.71 (1.69)	
10	6.32 (6.33)	
10a	3.23 (3.22)	2.52
10α		3.72
10β		1.86
11a		4.78
11b		4.87
1′	2.47 (2.46) [2.58][b]	2.47
2′	1.58 [1.61]	1.59
3′, 4′	1.37 [1.30–1.50]	1.32
5′	0.89 (0.89) [0.90]	0.89
1-OH	4.73 (4.87)	4.68

[a] Parenthetic values are from Archer *et al.* (16).
[b] Values in brackets are chemical shifts for *n*-pentyl benzene (17).

The remaining resonances, all of which belong to the C ring, were assigned on the basis of the coupling network identified in both the difference decoupling and 2D COSY experiments. Starting with H_{10a}, which couples through a vicinal mechanism only to H_{6a}, the network H_{10a} to H_{6a} to $H_{7\alpha}$ and $H_{7\beta}$ to $H_{8\alpha}$ and $H_{8\beta}$ was identified. The differentiation of the two 7 and 8, α and β, hydrogens was based on the values of their respective vicinal coupling constants.

Several ^{1}H NMR chemical shift assignments for $\Delta^{9,11}$-THC (the spectrum of which appears in Fig. 1b) were tentatively made by comparison with the assignments for Δ^9-THC, including those for the aromatic, methyl (6α-CH_3 and 6β-CH_3), and side-chain hydrogens, and were confirmed using decoupling and 2D COSY techniques. The olefinic hydrogens (11a and 11b) were differentiated on the basis of nOe enhancements. The remaining unassigned hydrogens belong to the C ring and were assigned using the same methods as used for Δ^9-THC. The coupling network is identified from $H_{10\alpha}$ and $H_{10\beta}$ through the intervening hydrogens and carbons of positions 10a, 6a, and 7, ending with hydrogens $H_{8\alpha}$ and $H_{8\beta}$. This network includes two additional hydrogens from an sp_3 hybridized carbon, as compared with Δ^9-THC, because the double bond is exocyclic in the $\Delta^{9,11}$-analog. This fact complicated the process of assigning the C ring resonances. However, both the COSY spectrum (Fig. 2) and the difference decoupling experiments were interpreted to give the same coupling network. Again, the 7 and 8, α and β, hydrogens were distinguished on the basis of vicinal coupling constants. The complete assignments for Δ^9-THC and $\Delta^{9,11}$-THC are summarized in Table 1.

Determination of Coupling Constants

^{1}H-^{1}H geminal (^2J) and vicinal (^3J) coupling constants. The 1D spectra of Δ^9- and $\Delta^{9,11}$-THC show that many resonances relevant to the conformational analysis overlap, precluding the determination of exact ^2J and ^3J values directly from these spectra. 2D *J*-resolved spectroscopy allows deconvolution of chemical shift and coupling constant information in spectra with overlapping peaks. We applied this method to determine approximate ^2J and ^3J values for both THC isomers using first-order analysis of the individual multiplets obtained as f_1 cross-sections in the 2D *J*-resolved spectra (shown for Δ^9-THC in Fig. 3). Fig. 4 shows the stacked plot representation of the entire 2D *J*-resolved spectrum for Δ^9-THC from which the cross-sections were derived.

These ^2J and ^3J values, along with the chemical shift values given in Table 1, were used as the starting point for an iterative simulation of subspectra containing all aliphatic resonances of the C ring of each molecule, using Bruker's LAOCOON (18, 19)-based PANIC software. The maximum number of spins the computer program can include in the calculation is eight. If all of the hydrogens of the C rings were included, counting the hydrogens at C_{11}, the number in both molecules exceeds eight. To eliminate this mismatch, we decoupled H_{10} in Δ^9-THC and H_{11a} and H_{11b} in $\Delta^{9,11}$-THC and then simulated these decoupled spectra. This procedure allowed for the determination of all geminal and vicinal coupling constants between aliphatic hydrogens of the C rings for each molecule. The decoupled spectra were acquired and calculations were performed at 250 MHz, due to the unavailability of the 500 MHz spectrometer during the period of time in which the analyses were performed. The experimental and calculated spectra for both molecules are

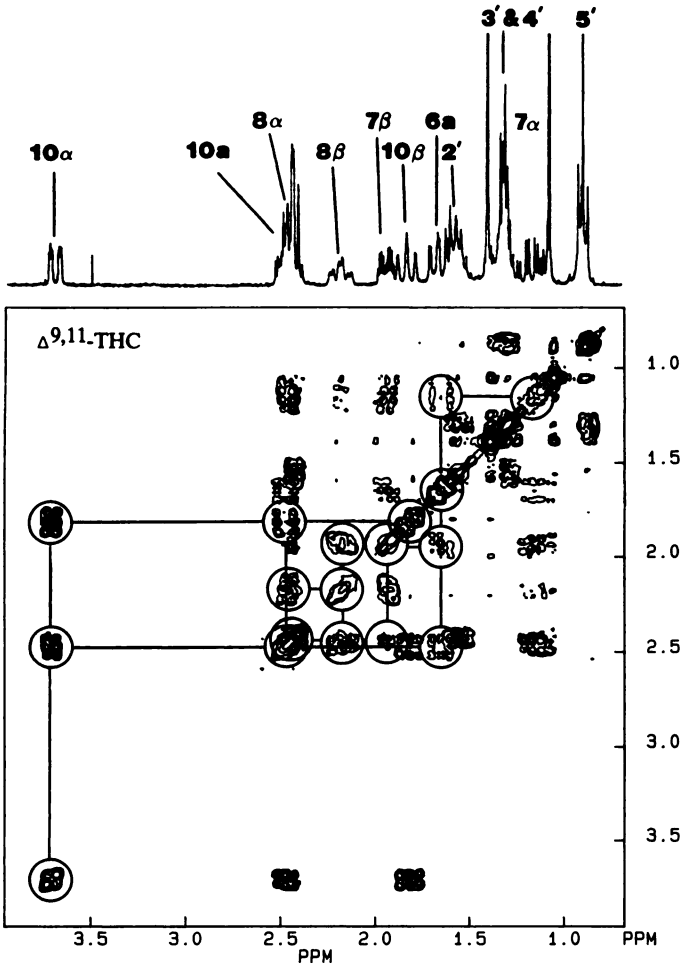

Fig. 2. Expanded scale contour plot of 250 MHz 2D COSY spectrum of aliphatic resonances of $\Delta^{9,11}$-THC. The *connected circles* indicate the coupling network identified for the C ring aliphatic resonances.

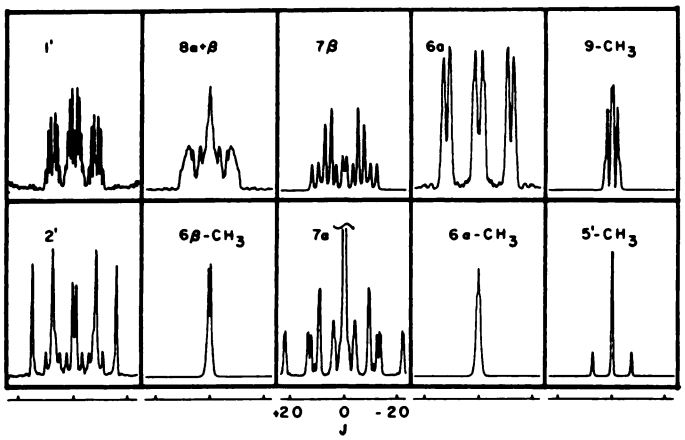

Fig. 3. *J* axis (f_1) cross-sections obtained from the 500 MHz 2D *J*-resolved ^{1}H NMR spectrum of Δ^9-THC.

shown in Figs. 5 and 6. The coupling constants so determined are summarized in Table 2.

Long range ^{1}H-^{1}H coupling constants. The existence of long range ^{1}H-^{1}H allylic (^4J), homoallylic (^5J), and "W" (^4J) coupling has been documented in a large number of organic molecules (20–25). We were interested in measuring such coupling constants from the ^{1}H NMR spectra of Δ^9-THC and $\Delta^{9,11}$-THC because their magnitudes are related to the relative geometries of the respective hydrogen atoms and, therefore, were useful for our conformational analyses. Because of their relatively small magnitudes, we were able to obtain only approximate ^4J and ^5J values. This was done by comparing $\Delta\nu_{1/2}$ values of peaks in the absence and presence of decoupling of one isolated hydrogen resonance involved in long range coupling and gives an approximate measure of the coupling constant. The method was used for hydrogens 8α, 8β, and 9-CH_3 coupling to H_{10} and H_{10a} in Δ^9-THC and hydrogens 8α, 8β, 10α, and 10β coupling to each other and to hydrogens 11a and 11b in $\Delta^{9,11}$-THC. 2D long range COSY experiments were performed to confirm the existence of the long range couplings observed, an example of which is shown for $\Delta^{9,11}$-THC in Fig. 7. The long range coupling constants measured using the above method for Δ^9-THC and $\Delta^{9,11}$-THC are summarized in Table 3.

^{13}C-^{1}H three-bond coupling constants. Three-bond ^{13}C-^{1}H coupling constants show Karplus-type angular dependence (26) and, thus, can be used to determine approximate dihedral angles between carbons and hydrogens separated by three single, sp_3-hybridized bonds. Using previously published ^{13}C chemical shift assignments for Δ^9-THC (27) and off-resonance ^{1}H-decoupled, single frequency ^{1}H-decoupled, and fully ^{1}H-coupled ^{13}C spectra obtained in our laboratories, we assigned the ^{13}C NMR chemical shifts of the 6α and 6β methyl groups and measured the coupling constants between the two methyl carbons and H_{6a} in Δ^9- and $\Delta^{9,11}$-THC. The chemical shifts and relevant coupling constants for the 6α and 6β methyl groups for Δ^9-THC and $\Delta^{9,11}$-THC are reported in Table 4.

^{1}H-^{1}H nOe

nOe enhancements can be used to determine the spatial relationships of hydrogens and are especially useful for the conformational analysis of rigid molecules (28). We measured nOe enhancements between the 6α- and 6β-CH_3 hydrogens and neighboring ring hydrogens in both cannabinoids. Preirradiation at subsaturating power levels was used to allow closely spaced peaks to be selectively irradiated. Also, difference techniques were used to enhance visualization of small nOe enhancements (1–5%) in overlapped regions of the spectra. These experiments were also useful in confirming the ^{1}H NMR assignments by Archer *et al.* (16) of the 6α-CH_3 and 6β-CH_3 resonances for Δ^9-THC and in determining the analogous assignments for $\Delta^{9,11}$-THC. In both isomers, enhancement of H_{10a} can only be accounted for upon irradiation of the 6α-CH_3, rather than the 6β-CH_3, due to the spatial disposition of these two groups. The assignments so determined are included in Table 1. The nOe enhancements measured for both molecules are reported in Table 5. Other nOe experiments were performed with preirradiation of the 1-OH in each isomer to determine the correct assignments of the two aromatic hydrogens and the preferred conformation around the phenol —OH bond. The resulting assignments are included in Table 1.

Discussion

We have combined several approaches for the conformational analysis of the tricyclic ring system in each of the two cannabinoid isomers. The C rings have multiple vicinal hydrogens and, therefore, were analyzed using the Karplus relationship to estimate interproton dihedral angles from vicinal ^3J values (6). The C ring conformations were initially obtained from the

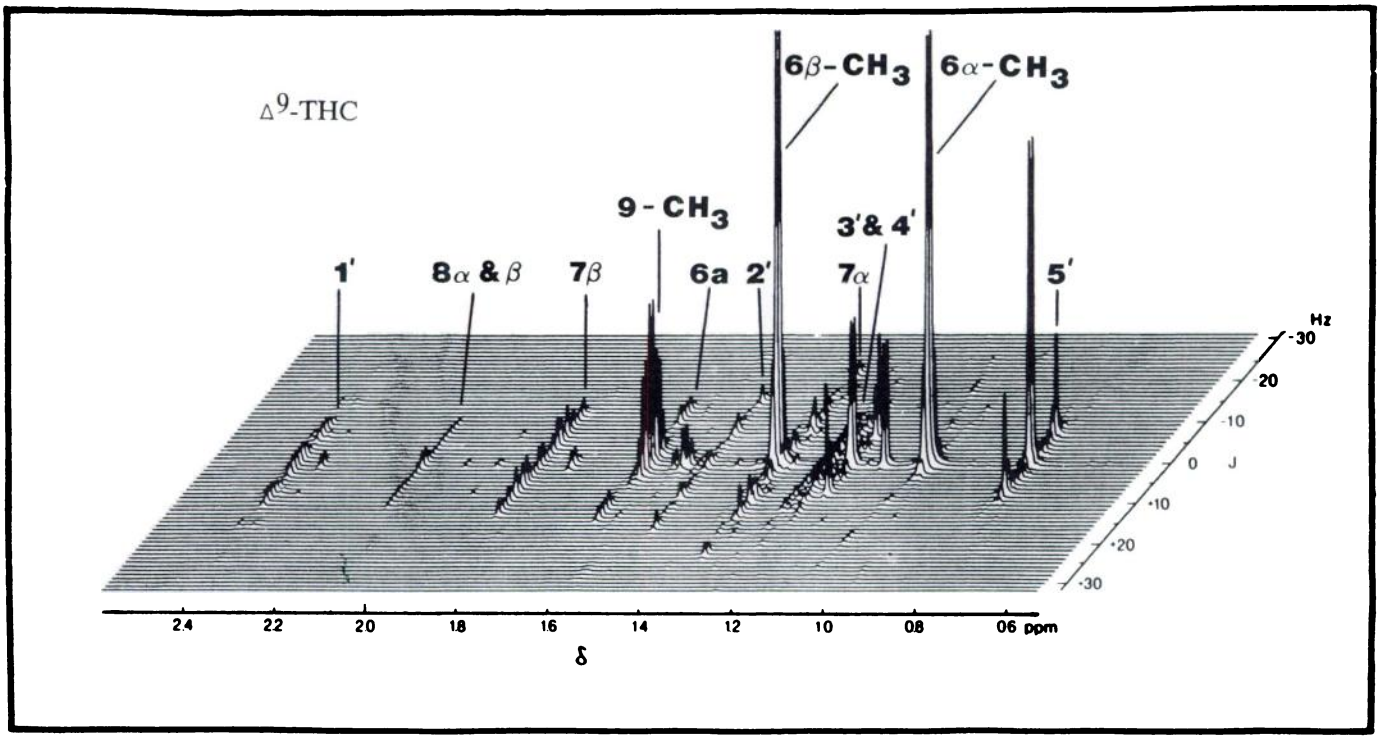

Fig. 4. Stacked plot of 500 MHz 2D *J*-resolved ^{1}H NMR spectrum of Δ^9-THC.

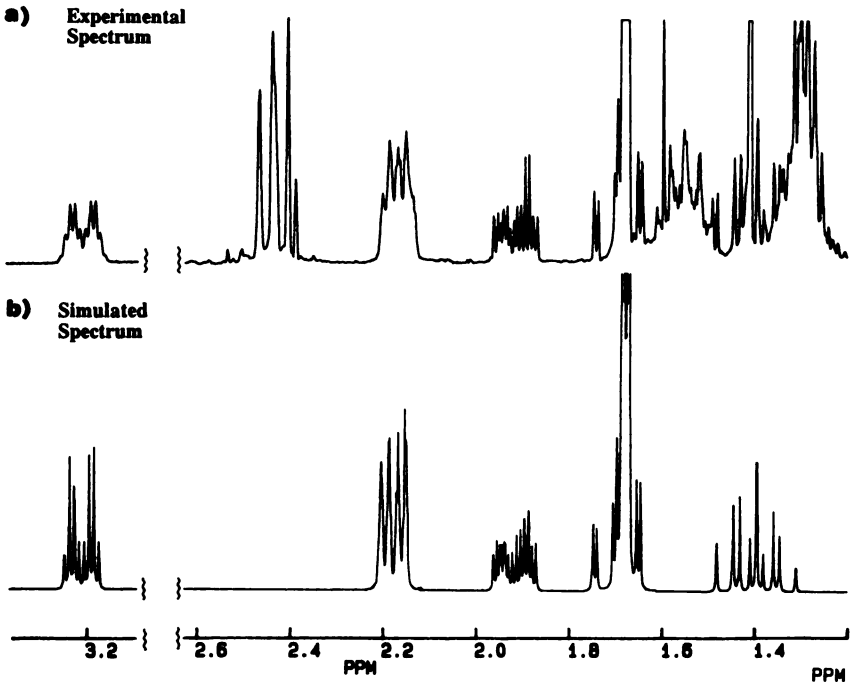

Fig. 5. Experimental (a) and simulated (b) 250 MHz ^{1}H NMR spectra of the aliphatic resonances of Δ^9-THC in which H-10 is decoupled (see text). Only the C ring resonances are simulated in b.

respective dihedral angles that overdetermine their geometries. Geometric information was also gained from the long range ^{1}H-^{1}H allylic (^4J), homoallylic (^5J), and W (^4J) coupling constants, which was then used to confirm the C ring conformation. The orientations of the two methyl groups in each of the B rings were obtained from the ^{13}C-^{1}H vicinal coupling constants and confirmed from the 6α- and 6β-CH_3 to H_{10a} nOe enhancement values. The orientation of the phenol —OH was determined from the respective nOe measurements. Finally, information on the preferred *n*-pentyl side-chain conformation was obtained from the long range coupling constants between the benzylic and aromatic hydrogens.

C ring. Central to the analysis of the conformation of the C ring in Δ^9- and $\Delta^{9,11}$-THC is the Karplus equation ($^3J = K\cos^2\theta$) (6), which relates the magnitude of vicinal coupling constants (^3J) to the dihedral angle (θ) between the coupled hydrogens. However, this equation must be used with caution (29, 30) because the value of K may vary and should be appropriately chosen for the molecular fragment under study. To obtain K values for each of the ^{1}H-^{1}H spin systems, we made use of vicinal coupling constants [$J(a\text{-}a)$, $J(a\text{-}e)$, $J(e\text{-}e)$]

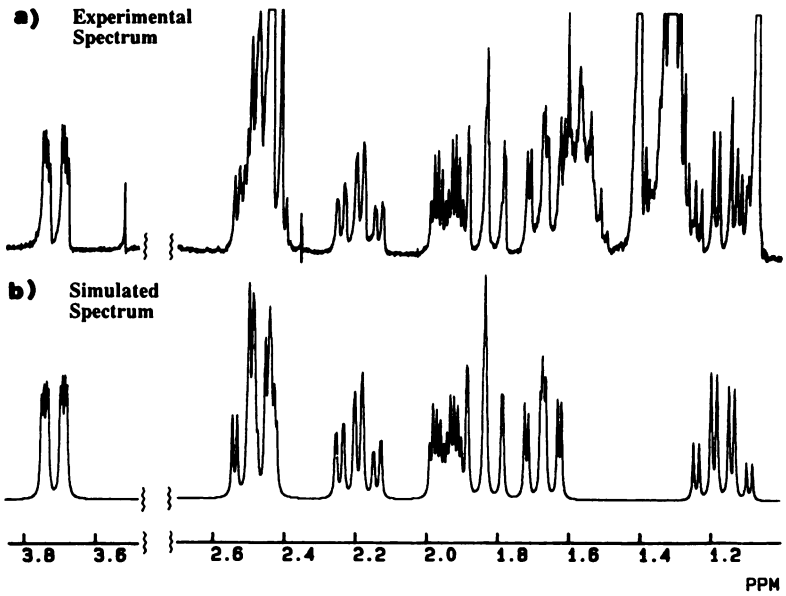

Fig. 6. Experimental (a) and simulated (b) 250 MHz ^{1}H NMR spectra of the aliphatic resonances of $\Delta^{9,11}$-THC in which H-11a and H-11b are decoupled (see text). Only the C ring resonances are simulated in b.

TABLE 2

^{1}H NMR geminal (^2J) and vicinal (^3J) coupling constants and dihedral angles determined for Δ^9- and $\Delta^{9,11}$-THC

Type of Coupling	Ha-Hb	Designation[a]	Δ^9-THC		$\Delta^{9,11}$-THC	
			n,*b*	Dihedral angle[c]	*n*,*b*	Dihedral angle[c]
			Hz		Hz	
Geminal	7α-7β	a-e	−12.6	[d]	−12.3	[d]
	8α-8β	a-e	−10.8	[d]	−13.5	[d]
	10α-10β	a-e		[d]	−13.0	[d]
Vicinal	6a-7α	a-a	12.5	166°	12.5	166°
	6a-7β	a-e	2.2	67°	2.7	64°
	6a-10a	a-a	10.7	154°	11.0	155°
	7α-8α	a-e	7.7	43°	4.0	58°
	7α-8β	a-a	10.4	152°	13.0	171°
	7β-8α	e-e	2.8	61°	2.2	65°
	7β-8β	e-a	5.4	52°	5.3	53°
	10a-10α	a-e			3.3	61°
	10a-10β	a-a			11.8	160°
	10-10a		1.8	≈90°		

[a] These designations refer to the relative orientation of the two involved hydrogens: a-e, axial-equatorial; etc.

[b] Determined from simulations of spectra obtained at 250 MHz, n=2 for geminal coupling, n=3 for vicinal coupling.

[c] Calculated using the equation $^3J = K\cos^2\theta$, where $K_{a\text{-}a}$ = 13.31 Hz, $K_{a\text{-}e}$ = $K_{e\text{-}a}$ = 14.36 Hz, and $K_{e\text{-}e}$ = 12.24 Hz; θ is the dihedral angle; K values were calculated using ^3J values measured in 1,1′,4,4′-tetradeuterocyclohexane (31) and dihedral angles determined for cyclohexane (30).

[d] These bond angles cannot be quantitatively determined because many electronic and geometric factors contribute to the magnitude of ^2J, making quantitative correlations between ^2J and bond angle impractical (30).

[e] This vicinal coupling involves an sp_2-hybridized carbon but still obeys the Karplus relationship. The small magnitude of ^3J indicates an angle near 90° (30).

measured in 1,1′,4,4′-tetradeuterocyclohexane at low temperatures (31) along with independently determined corresponding dihedral angles for cyclohexane (30).

Δ^9-THC. The values of dihedral angles given in Table 2 are consistent with a chair conformation flattened in the C_8-C_9-C_{10} region of the ring. As a starting point for our analysis, we chose H_{6a}, which must have a *trans* diaxial relationship with respect to H_{10a}. The large value of $^3J(H_{6a}\text{-}H_{7\alpha})$ identifies $H_{7\alpha}$ as axial with respect to H_{6a}, whereas $H_{7\beta}$ is equatorial. Our calculations find that the dihedral angles between the $H_{7\alpha}$, $H_{7\beta}$, $H_{8\alpha}$, and $H_{8\beta}$ C ring hydrogens (152°, 43°, 52°, 61°) differ considerably from the almost perfectly staggered conformation in cyclohexane (175°, 55°, 55°, 65°) (30) but have a closer resemblance to the corresponding angles in cyclohexene (160°, 40°, 40°, 80°) (32). The value for the $H_{8\alpha}$-$H_{8\beta}$ geminal coupling constant (^2J = −10.8 Hz) is smaller than that expected for an sp_3-hybridized methylene group ($^2J \approx -12.5$ Hz) (29) and may reflect a decrease in the corresponding $H_{8\alpha}$-C_8-$H_{8\beta}$ bond angle, which is also in accord with a half-chair C ring conformation. On the other hand, the H_{6a}-H_{10a} ^3J (*a*-*a*) value (^3J = 10.7 Hz) is relatively small and, according to our calculations, leads to a dihedral angle smaller than that for perfectly staggered *trans* diaxial hydrogens. This can be attributed to the effect of the neighboring phenyl ring, which has been shown to reduce the value of a ^{1}H-^{1}H vicinal coupling, leading to an underestimated value for the corresponding dihedral angle. The above conclusions on the C ring conformation of Δ^9-THC are further supported by our data for allylic couplings between $H_{8\alpha}$ and $H_{8\beta}$ and the olefinic H_{10} (Table 3). The values for these long range couplings (0.9, 0.9 Hz) are smaller than the expected maximum value ($^4J \approx 3$ Hz) for allylic hydrogens at a 90° angle with respect to the plane of the double bond (21). These values correspond to approximately 45° angles and indicate that the plane of the C_9-C_{10} double bond bisects the $H_{8\alpha}$-C_8-$H_{8\beta}$ bond angle.

We have considered the possibility of the existence of a dynamic equilibrium between two or more conformers involving flexibility in the C_7-C_8 segment of the C ring but have ruled this out based on the following evidence. Flexibility in this ring of Δ^9-THC would most likely lead to an equilibrium between the flattened chair and the flattened boat conformers. The existence of a significant population of the flattened boat conformer is precluded by the observation of a large value for $^3J(H_{6a}\text{-}H_{7\alpha})$ (12.5 Hz); this is representative of a *trans* diaxial orientation for these two hydrogens. In a flattened boat conformer, this ^3J value would be approximately 4 Hz and, in the equilibrium situation, would be averaged to some value between the maximum value of 12.5 Hz and the minimum value of 4 Hz.

$\Delta^{9,11}$-THC. The ^{1}H-^{1}H vicinal coupling constants for the C ring indicate a chair conformation resembling that of cyclohexane. This conclusion is supported by the ^{1}H-^{1}H long range

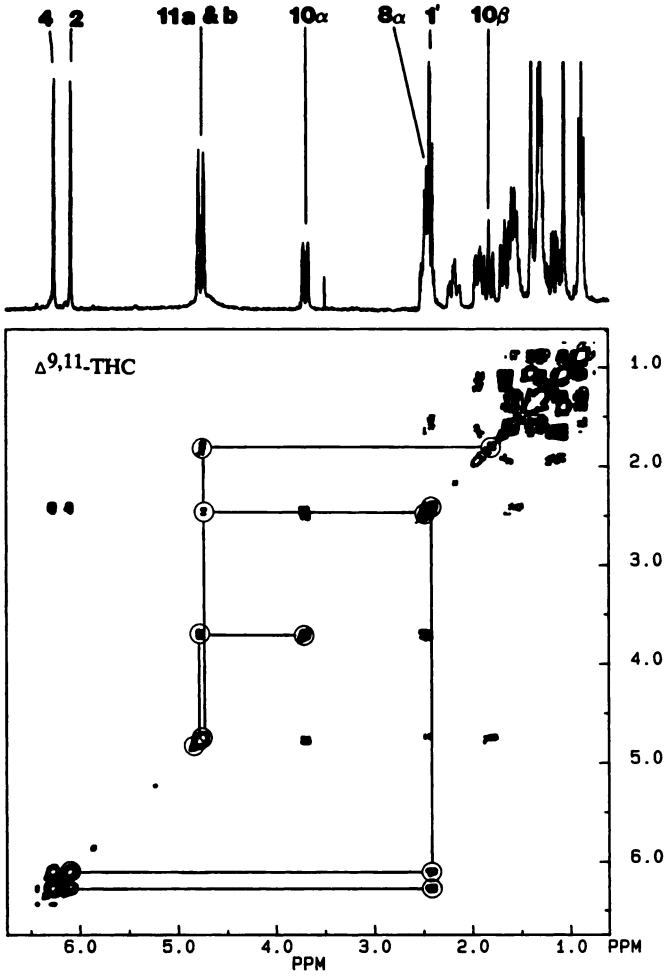

Fig. 7. Contour plot of 250 MHz 2D long range COSY spectrum of $\Delta^{9,11}$-THC with long range coupling to the aromatic protons indicated in the *lower right* region of the spectrum and long range coupling to the olefinic protons indicated in the *upper left* region.

coupling constant data (Table 3), which include (a) a W coupling between $H_{8\alpha}$ and $H_{10\alpha}$ (^4J = 1.5 Hz), indicating a planar or nearly planar $H_{8\alpha}$-C_8-C_9-C_{10}-$H_{10\alpha}$ segment (20, 29); (b) four allylic couplings between $H_{8\beta}$ and $H_{10\beta}$ and H_{11a} and H_{11b} (1.5, 1.9, 1.7, 1.5 Hz), indicating that $H_{8\beta}$ and $H_{10\beta}$ are perpendicular or nearly perpendicular to the plane of the C_9-C_{11} double bond (21); (c) absence of coupling between $H_{8\alpha}$ and $H_{10\alpha}$ and the two vinyl hydrogens, indicating that $H_{8\alpha}$ and $H_{10\alpha}$ line in or nearly in the plane of the double bond (21). As in the case of Δ^9-THC above, the existence of a significant population of other conformers for $\Delta^{9,11}$-THC is ruled out by the observation of large, unaveraged, vicinal interproton coupling constants within the C ring.

B Ring. In Δ^9- and $\Delta^{9,11}$-THC the B ring, due to the possibility for flexibility about the C_6-C_{6a} bond, can assume either the conformation of a distorted chair in which the 6α-CH_3 is pseudoaxial and the 6β-CH_3 is pseudoequatorial or that of a distorted boat in which the 6α-CH_3 is now pseudoequatorial and the 6β-CH_3 is pseudoaxial. As a basis for our conformational analysis, we have selected ^{13}C-^1H coupling constants (Table 4) and found a close resemblance between the B rings of both molecules. These three-bond coupling constants obey a Karplus-type relationship having a maximum value (4.0–5.5 Hz) for dihedral angles of 180° and 0° and near zero values for

TABLE 3

^1H NMR long range coupling constants and interproton angular relationships determined for Δ^9- and $\Delta^{9,11}$-THC

Type of Coupling	H_a-H_b	Δ^9-THC		$\Delta^{9,11}$-THC	
		n,[a]	Interpretation[b]	n,[a]	Interpretation
		Hz		Hz	
W, ^4J	8α-10α			1.5	Planar[c]
	8α-10β			<0.2	Nonplanar
	8β-10α			<0.2	Nonplanar
	8β-10β			<0.2	Nonplanar
Allylic, ^4J	8α-10	0.9	50°[d]		
	8β-10	0.9	50°		
	9-CH_3-10	1.6	None		
	8α-11a			<0.2	0°[d]
	8α-11b			<0.2	−20°
	8β-11a			1.5	135°
	8β-11b			1.9	110°
	10α-11a			0.3	0°
	10α-11b			0.3	0°
	10β-11a			1.7	120°
	10β-11b			1.5	135°
Benzylic, ^4J	2-1′	0.5	±30°[e]	0.6	30°[e]
	4-1′	0.7	±30°	0.7	30°
Aromatic, ^4J	2-4	1.7	[f]	1.7	[f]
Homoallylic, ^5J	8α-10a	1.5			
	8β-10a	1.5			
	$H_{8\alpha}$-C_8-C_9-C_{10} and $H_{8\beta}$-C_8-C_9-C_{10}		50°[g]		
	H_{10a}-C_{10a}-C_{10}-C_9		90°		

[a] n is the number of bonds through which coupling occurs.
[b] All angular values reported are ±10°.
[c] W couplings are observed when the involved hydrogens are coplanar, with the two dihedral angles equalling or nearly equalling 180°. In this case the $H_{8\alpha}$-C_8-C_9-C_{10}-$H_{10\alpha}$ segment is coplanar (20).
[d] These dihedral angles are approximated from Tables 11 and 12 of Ref. 21, which show the best fit of experimentally determined $^4J_{allylic}$ values and dihedral angles to theoretical calculations.
[e] These dihedral angles between the benzylic CH bond and the plane of the aromatic ring are based on the $^4J_{benzylic} = {}^4J_{90°} \sin^2\theta$ relationship, where $^4J_{90°}$ equaled 2.4 Hz (23).
[f] Geometry fixed in aromatic ring.
[g] Determined from the known $\sin^2\theta$ dependence of ^5J (22) and the fixed geometry of H_{10a}.

TABLE 4

^{13}C NMR chemical shift and ^{13}C-^1H coupling constant values determined for the 6α-CH_3 and 6β-CH_3 for Δ^9- and $\Delta^{9,11}$-THC

Methyl Carbon	Chemical Shift[a]		Proton	Coupling Constant $n_{J_{CH}}$,[b]		
	Δ^9-THC	$\Delta^{9,11}$-THC		Δ^9-THC	$\Delta^{9,11}$-THC	n
	ppm			Hz		
6α	19.06	19.04	$H_{6\alpha}$	126.0	126.0	1
			$H_{6\beta}$	4.2	4.2	3
			H_{6a}	4.0	4.2	3
6β	27.80	27.78	$H_{6\beta}$	130.0	126.0	1
			$H_{6\alpha}$	3.8	3.8	3
			H_{6a}	<0.6	<0.6	3

[a] Spectra obtained at 125 MHz using TMS at 0.0 ppm as internal reference.
[b] n is the number of bonds through which coupling occurs.

90° and 270° angles (6, 26). We found ^3J between H_{6a} and $C_{6\beta}$ to be nearly zero, corresponding to a H_{6a}-C_{6a}-C_6-$C_{6\beta}$ angle close to 90° and a relatively large value for ^3J between H_{6a} and $C_{6\alpha}$ corresponding to a H_{6a}-C_{6a}-C_6-$C_{6\alpha}$ angle of approximately 180°. The data, therefore, show the 6α-CH_3 to be psuedoaxial and the 6β-CH_3 pseudoequatorial, corresponding to a distorted chair conformation. As in the case of the C ring, we have considered the possibility that our data represent a dynamic equilibrium

TABLE 5
nOe enhancements measured for Δ^9- and $\Delta^{9,11}$-THC

Resonance Irradiated	Resonance Observed	nOe Enhancements	
		Δ^9-THC	$\Delta^{9,11}$-THC
		%	
6α-CH_3	6β-CH_3	5	5
	H_{6a}	0	0
	H_{10a}	6	13
6β-CH_3	6α-CH_3	4	5
	H_{6a}	4	2
	H_{10a}	0	0
1-OH	H_2	7	7
	H_4	0	0

between the distorted chair and distorted boat conformers. However, the observation of both the maximum and minimum values for the respective vicinal ^{13}C-^1H coupling constants, rather than averaged intermediate values for both, eliminate this as a likely explanation.

We have used nOe measurements to confirm the above conclusions, including the consideration of dynamic processes. Irradiation of the 6α-CH_3 in Δ^9-THC leads to nOe enhancements of 5% in the 6β-CH_3 and 6% in H_{10a} (Table 5). These results indicate that the 6α-CH_3 is in close spatial proximity to H_{10a}, with an axial or nearly axial orientation. Irradiation of the 6β-CH_3 was complicated by the fact that $H_{7\alpha}$ partly overlaps this resonance, leading to artifacts in the nOe enhancements measured, which, therefore, cannot be meaningfully interpreted and were omitted from Table 5. In $\Delta^{9,11}$-THC, a relatively large nOe enhancement is seen in H_{10a} (13%) when the 6α-CH_3 is irradiated, whereas no enhancement in H_{10a} is observed upon irradiation of the 6β-CH_3. This indicates that the 6α-CH_3 is axial, or nearly so, and spatially near H_{10a}.

Again, the existence of an equilibrium situation must be considered, especially when conclusions are based on interpretations of nOe results. The intensity of nOe enhancements vary as $1/r^6$ (where r is the ^1H-^1H internuclear distance) and are heavily weighted by contributions from hydrogens having relatively short internuclear distances (28). In the case of a dynamic equilibrium, a minor conformer can contribute significantly to observed nOe enhancements if, in this conformer, the ^1H-^1H distance is short. In the case of the two THC isomers discussed here, we have eliminated such an explanation based on the observation that any nOe enhancements that would be expected for hydrogens having short internuclear distances in a distorted boat conformer are absent in our nOe spectra. For example, a strong enhancement of $H_{7\beta}$ upon irradiation of the 6α-CH_3 would be expected in a distorted boat conformer for both Δ^9- and $\Delta^{9,11}$-THC. However, this enhancement is not observed.

A ring. Information on the orientation of the phenol hydroxyl group at position 1, as well as confirmation of the chemical shift assignments for H_2 and H_4, was obtained from the nOe enhancement values of neighboring hydrogens upon irradiation of the former resonance. For Δ^9-THC, there was an enhancement of 7% in H_2 and no enhancement in H_{10} (or H_4), indicating that the 1-OH is oriented towards H_2. With $\Delta^{9,11}$-THC, irradiation of the 1-OH also gives only one enhancement of 7% at H_2, indicating that this group is also oriented towards H_2.

Pentane Side-Chain. The conformation of the flexible *n*-pentane side-chain was analyzed using the values of benzylic ^1H-^1H coupling constants (H_2 and H_4 to 1′-CH_2) reported in Table 3. Attempts were made to accurately determine these values using simulation methods applied to 250 MHz ^1H NMR spectra but these were unsuccessful because of our inability to distinguish between contributions to line widths from long range coupling, natural line width, and magnetic field inhomogeneities. The approximate coupling constant values reported in Table 3 were determined using the method of line width difference in the absence and presence of decoupling. According to theory (25), the magnitude of benzylic coupling constants is greatest (−1.5 Hz) when the aliphatic CH bond is perpendicular to the plane of the aromtic ring and is at a minimum (−0.4 Hz) when the CH bond lies in the plane of the aromatic ring. In our spectra, we found that the absolute values of coupling constants range between 0.5 and 0.7 Hz (±0.1 Hz) (Table 3). These have not been determined with suitable accuracy to allow an exact computation of the benzylic dihedral angles ($H_{1'}$-$C_{1'}$-C_3-C_2-H_2 and $H_{1'}$-$C_{1'}$-C_3-C_4-H_4). However, they provide us with approximate information on the conformation around the C_3-$C_{1'}$ bond. Based on the theoretical guidelines provided by Wasylishen and Schaefer (25) and the experimental results of Giessner-Prettre and Pullman (23), the data rule out a conformation in which one of the $C_{1'}$-$H_{1'}$ bonds is coplanar with the aromatic ring and show that the most likely conformation is one in which the two benzylic hydrogens form angles of approximately 30° and −30° with the aromatic ring and the $C_{1'}$-$C_{2'}$ bond is perpendicular to the aromatic ring. These data, however, do not rule out the possibility for an interpretation involving the dynamic averaging of several conformers, leading to the intermediate ^4J values observed. However, our proposed conformation is in agreement with the one observed in the crystal form for other related cannabinoid analogs (33, 34). Unfortunately, neither Δ^9- nor $\Delta^{9,11}$-THC yield crystals for X-ray studies.

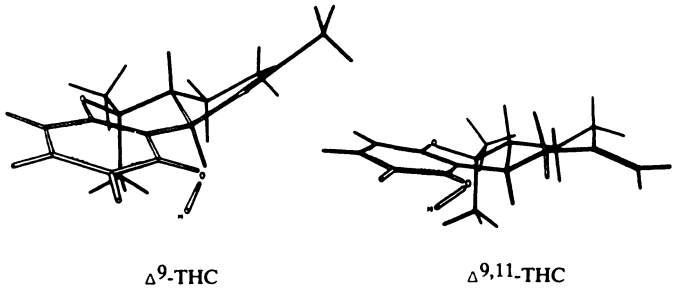

Δ^9-THC $\Delta^{9,11}$-THC

Fig. 8. Drawings showing the experimentally determined conformations for Δ^9-THC and $\Delta^{9,11}$-THC.

Conclusions

Our data show that Δ^9- and $\Delta^{9,11}$-THC have similar B ring and side-chain conformations. However, they show considerable variation in the C rings. In Δ^9-THC, the C ring assumes a somewhat flattened chair conformation, causing the 9-CH_3 to project *above* the plane of the aromatic ring. On the other hand, the C ring of $\Delta^{9,11}$-THC adopts a chair conformation, as found in cyclohexane. This conformation projects the exocyclic methylene group *into* the plane of the aromatic ring and places all three rings in a coplanar geometry (Fig. 8).

It is tempting to postulate that the observed conformational differences between Δ^9-THC and its $\Delta^{9,11}$- analog may serve to

explain the large pharmacological differences between these two cannabinoids and that the deviation from planarity in the tricyclic ring system of the pharmacologically active Δ^9- isomer may be a requirement for activity. We have made analogous observations in the case of anesthetic steroids (35, 36). Both the anesthetic steroids and the cannabinoids are believed to produce their pharmacological effects, at least in part, through interactions with cellular membranes. Such an argument would also explain the lack of activity of cannabinol, a cannabinoid with aromatic A and C rings and a planar tricyclic system.

We have explained the differences in activity between nonplanar and planar steroid analogs by invoking an interaction of the nonplanar active steroid with the membrane bilayer that results in membrane perturbation. On the other hand, the planar steroid, because of its geometry, fails to perturb the membrane. Indeed, we have shown this to be the case, using model membranes, with the help of high resolution and solid state NMR spectroscopy (36, 37). An analogous interpretation can be used to explain the differences in activities between the two cannabinoids described in this communication. This hypothesis is supported by some recent data from our laboratory comparing the effects of Δ^9-THC and $\Delta^{9,11}$-THC on model membranes using ^2H solid state NMR spectroscopy. The experiments showed that, indeed, the pharmacologically active Δ^9-THC perturbs the model membrane more effectively than the inactive $\Delta^{9,11}$-THC (38). An alternative hypothesis for the mechanism of action of the cannabinoids in that these molecules induce their effects by interacting with a specific membrane-associated functional protein. If this proves to be true, our data would indicate that a flat cannabinoid structure with all the rings coplanar does not allow for a productive binding of the drug with the active site and that an out-of-plane C ring induces a more favorable interaction. Currently, we are continuing these studies with other cannabinoid analogs in an effort to further understand the molecular requirements for cannabinoid activity.

Acknowledgments

The authors would like to thank members of the NMR laboratory of Boehringer Ingelheim Pharmaceuticals, Inc. (Dr. Phil Pitner, Mr. Scott Leonard, and Ms. Tracy Saboe) and Dr. F. K. Hess (Director, Department of Analytical Sciences, BIPI) for assistance and helpful discussion during the preparation of this manuscript.

References

1. Razdan, R. K. Structure-activity relationships in cannabinoids. *Pharmacol. Rev.* **38**:75–149 (1986).
2. Agurell, S., M. Halldin, J.-E. Lindgren, A. Ohlsson, M. Widman, H. Gillespie, and L. Hollister. Pharmacokinetics and metabolism of Δ^9-THC and other cannabinoids with emphasis in man. *Pharmacol. Rev.* **38**:21–43 (1986).
3. Martin, B. R. Cellular effects of cannabinoids. *Pharmacol. Rev.* **38**:45–74 (1986).
4. Agurell, S., W. L. Dewey, and R. E. Willelte, eds. *The Cannabinoids; Chemical, Pharmacologic, and Therapeutic Aspects.* Academic Press, New York (1987).
5. Mechoulam, R., and E. Edery. Structure-activity relationships in the cannabinoid series, in *Marihuana: Chemistry, Pharmacology, Metabolism, and Clinical Effects* (R. Mechoulam, ed.). Academic Press, New York, 101–136 (1973).
6. Karplus, M. Contact electron-spin coupling of nuclear magnetic moments. *J. Chem. Phys.* **30**:11–15 (1959).
7. Hall, L. D., and J. K. M. Sanders. Complete analysis of ^1H NMR spectra of complex natural products using a combination of one- and two-dimensional techniques: 1-dehydrotestosterone. *J. Am. Chem. Soc.* **102**:5703–5711 (1980).
8. Muller, L., A. Kumar, and R. R. Ernst. Two-dimensional carbon-13 NMR spectroscopy. *J. Chem. Phys.* **63**:5490–5491 (1975).
9. Aue, W. P., J. Karhan, and R. R. Ernst. Homonuclear broadband decoupling and two-dimensional *J*-resolved NMR spectroscopy. *J. Chem. Phys.* **64**:4226–4227 (1976).
10. Bodenhausen, G., R. Freeman, and D. L. Turner. Suppression of artifacts in two-dimensional J spectroscopy. *J. Magn. Reson.* **27**:511–514 (1977).
11. Hoult, D. I., and R. E. Richards. Critical factors in the design of sensitive high resolution nuclear magnetic resonance spectrometers. *Proc. R. Soc. A* **344**:311–340 (1975).
12. Aue, W. P., E. Bartholdi, and R. R. Ernst. Two-dimensional spectroscopy: application to nuclear magnetic resonance. *J. Chem. Phys.* **64**:2229–2246 (1976).
13. Bax, A., R. Freeman, and G. A. Morris. Correlation of proton chemical shifts by two-dimensional Fourier transform NMR. *J. Magn. Reson.* **42**:164–168 (1981).
14. Nagayama, K., A. Kumar, K. Wuthrich, and R. R. Ernst. Experimental techniques of two-dimensional correlated spectroscopy. *J. Magn. Reson.* **40**:321–334 (1980).
15. Bax, A., and R. Freeman. Investigation of complex networks of spin-spin coupling by two-dimensional NMR. *J. Magn. Reson.* **44**:542–561 (1981).
16. Archer, R. A., D. B. Boyd, P. V. Demarco, I. J. Tyminski, and N. L. Allinger. Structural studies of cannabinoids: a theoretical and proton magnetic resonance analysis. *J. Am. Chem. Soc.* **92**:5200–5206 (1970).
17. *Stadtler Standard Spectra.* Ref. No. 3613 M, Stadtler Research Laboratories, Philadelphia (1967).
18. Diehl, P., H. Kellerhals, and E. Lustig. Computer assistance in the analysis of high-resolution NMR spectra, in *NMR: Basic Principles and Progress* (P. Diehl, E. Fluck, and R. Kosfeld, eds.). Springer-Verlag, New York, 1–96 (1972).
19. Castellano, S. in *Computer Programs for Chemistry* (P. E. De Tar, ed.). Benjamin Press, New York, 1–25 (1968).
20. Barfield, M., and B. Chakrabarti. Long-range proton spin-spin coupling. *Chem. Rev.* **69**:757–778 (1969).
21. Barfield, M., R. J. Spear, and S. Sternhell. Allylic interproton spin-spin coupling. *Chem. Rev.* **76**:593–624 (1976).
22. Barfield, M., and S. Sternhell. Conformational dependence of homoallylic H-H coupling constants. *J. Am. Chem. Soc.* **94**:1905–1913 (1972).
23. Griessner-Prettre, C., and B. Pullman. Molecular-orbital study of the orthobenzylic long-range proton-proton coupling constants $^4J_{HH}$ in biological phenethyl amines. *J. Magn. Reson.* **18**:564–568 (1975).
24. Lambert, F., M. Ellenberger, L. Merlin, and Y. Cohen. NMR study of catechol and catechol amines. *Org. Magn. Reson.* **7**:266–273 (1975).
25. Wasylishen, R., and T. Schaefer. INDO molecular orbital calculations on the conformational dependence of long-range spin-spin coupling of methyl protons in toluene, *p*-fluorotoluene, and the xylenes. *Can. J. Chem.* **50**:1852–1862 (1972).
26. Hansen, P. E. Carbon-hydrogen spin-spin coupling constants. *Prog. NMR Spectrosc.* **14**:175–296 (1981).
27. Wenkert, E., D. W. Cochran, F. M. Schell, R. A. Archer, and K. Matsumoto. Carbon-13 nuclear magnetic resonance (CMR) spectroscopy of naturally occurring substances. IX. CMR spectral analysis of tetrahydrocannabinol and its isomers. *Experientia (Basel)* **28**:250–261 (1972).
28. Noggle, J. H., and R. E. Schirmer. *The Nuclear Overhauser Effect.* Academic Press, New York, (1971).
29. Jackson, L. M., and S. Sternhell. *Applications of Nuclear Magnetic Resonance Spectroscopy in Organic Chemistry.* Pergamon Press, New York, (1969).
30. Booth, H. Applications of hydrogen nuclear magnetic resonance spectroscopy to the conformational analysis of cyclic compounds. *Prog. NMR Spectrosc.* **5**:149–381 (1969).
31. Garbisch, E. W., and M. G. Griffith. Proton couplings in cyclohexane. *J. Am. Chem. Soc.* **90**:6543–6544 (1968).
32. Gunther, H., and G. Jekeli. ^1H Nuclear magnetic resonance spectra of cyclic monoenes: hydrocarbons, ketones, heterocycles, and benzo derivatives. *Chem. Rev.* **77**:599–637 (1977).
33. Ottersen, T., E. Rosenqvist, C. E. Turner, and F. S. El-Feraly. The crystal and molecular structure of cannabidiol. *Acta Chem. Scand. Ser. B Org. Chem. Biochem.* **31**:807–812 (1977).
34. Jones, P. G., L. Falvello, O. Kennard, G. Sheldrick, and R. Mechoulam. Cannabidiol. *Acta Crystallogr. Sect. B Struct. Crystallogr. Cryst. Chem.* **B33**:3211–3214 (1977).
35. Makriyannis, A., and S. W. Fesik. Mechanism of steroid anesthetic action: interactions of alphaxalone and Δ^{16}-alphaxalone with bilayer vesicles. *J. Med. Chem.* **26**:463–465 (1983).
36. Fesik, S. W., and A. Makriyannis. Geometric requirements for membrane perturbation and anesthetic action. *Mol. Pharmacol.* **27**:624–629 (1985).
37. Makriyannis, A., D. J. Siminovitch, S. K. Das Gupta, and R. G. Griffin. Studies on the interaction of anesthetic steroids with phosphatidylcholine using deuterium and carbon-13 solid state NMR. *Biochim. Biophys. Acta* **859**:49–55 (1986).
38. Makriyannis, A., A. Banijamali, C. J. Van der Schyf, and H. Jarrell. Interactions of cannabinoids with membranes: the role of stereochemistry and absolute configuration and the orientation of *delta*-9-THC in the membrane bilayer, in *Structure-Activity Relationships of Cannabinoids* (R. Rapaka and A. Makriyannis, eds). NIDA Research Monograph No. 79, Bethesda, MD, 123–133 (1987).

Send reprint requests to: Richard W. Kriwacki, Boehringer Ingelheim Pharmaceuticals, Inc., Dept. of Analytical Sciences, 90 East Ridge, Ridgefield, CT 06877.